Catalysis Science & Technology

ROYAL SOCIETY OF CHEMISTRY

PAPER

View Article Online
View Journal | View Issue

Check for updates

Cite this: *Catal. Sci. Technol.*, 2025, **15**, 2551

Adsorbed O promotes alternative, nonselective oxametallacycle reaction pathways in Ag-catalyzed epoxidation†

Shengjie Zhang,‡ Sarah M. Stratton‡ and Matthew M. Montemore *

Received 10th December 2024,
Accepted 2nd March 2025

DOI: 10.1039/d4cy01486c

rsc.li/catalysis

Ethylene oxide (EO) is a vital compound used as an intermediate in the production of other important compounds, such as ethylene glycol and glycol ether. EO is produced by selective ethylene oxidation (epoxidation) over supported Ag catalysts. Achieving high selectivity is the primary goal of research in this area, and understanding the factors that influence selectivity is thus critical for improving performance. The most widely accepted intermediate in EO production is the oxametallacycle (OMC). However, possible reactions between surface O and the OMC have not been comprehensively studied. In this work, density functional theory was used to systematically study the possible reaction pathways from the OMC in the presence of surface O. We find that surface O opens up two kinetically and thermodynamically favorable pathways that have received little or no attention in previous studies, neither of which form EO. Specifically, O-assisted C–H bond scission and the formation of ethylenedioxy are quite facile and predicted to be more favorable than the traditional EO (ring-closure) and acetaldehyde (H transfer) pathways. Thus, the predicted selectivity in the presence of coadsorbed O is very low, less than 0.1% at typical reaction temperatures. Furthermore, surface O has a similar effect on the propylene-derived OMC, which may have relevance to propylene oxidation. These results show the potential importance of surface O in influencing selectivity, as surface O greatly promotes these non-selective reactions and should therefore be minimized. These O-promoted reaction pathways should be considered in both design and kinetic modelling of EO catalysts.

1. Introduction

Ethylene oxide (EO) is an important chemical with a wide range of applications such as sterilizing agents, fumigants and blowing agents in foam production. More importantly, it is an essential intermediate in the chemical industry that can be converted into many other chemicals of interest, such as ethylene glycol, a key ingredient of antifreeze and coolants, and glycol ether, which is used in paints and cleaning products.[1] In 2022, the global market volume of EO was 31.6 million metric tons, with a market value of $51.7 billion. The market volume is forecasted to grow to more than 37 million metric tons and its market value is projected to reach $91 billion in 2032.[2,3] Meanwhile, EO production generates 0.4 tons of CO_2 per ton of product, making it one of the chemical industry's largest contributors to carbon emissions.[4] This suggests that improvements in EO production techniques, particularly with respect to selectivity, could lead to enormous benefits for energy and the environment. Similarly, there is great interest in the improvement of propylene oxide (PO) industrial production because of PO's role in the manufacturing of polyurethane foams that are used in the production of bedding, furniture, automotive interiors, and many other products that are used daily.[5,6]

In industry, EO is produced by selective oxidation of ethylene over supported Ag-based catalysts. While millions of tons of EO are produced yearly, the nature of the catalytic process is not fully understood, leading to ongoing and significant efforts into understanding the mechanism and design principles.[7] The primary goal of these investigations is to reach higher conversion and, most importantly, higher selectivity towards EO. Additionally, PO production *via* the epoxidation of propylene has proved to be a particularly challenging reaction for heterogenous catalysts, which usually suffer from poor selectivity.[8] Many current studies on Ag-catalyzed ethylene oxidation focus on the surface conditions of the catalyst,[9–15] the ethylene oxidation mechanism itself,[16–29] and the role of various promoters.[7,30–38] Despite intensive research, there are still some critical questions related to the mechanism that remain unclear. In this work, we examine the mechanism and

Department of Chemical and Biomolecular Engineering, Tulane University, New Orleans, Louisiana 70118, USA. E-mail: mmontemore@tulane.edu

† Electronic supplementary information (ESI) available. See DOI: **https://doi.org/10.1039/d4cy01486c**

‡ These two authors contributed equally to this work.

propose overlooked possible pathways that are more likely to occur than traditionally studied pathways if coadsorbed O is present.

The most widely accepted intermediate for ethylene oxidation on Ag surfaces is an oxametallacycle (OMC).[16,17,39] Two somewhat different OMC configurations with similar energies have been studied, one where the C and O share an Ag atom and one in which the C and O are bound to separate Ag atoms.[17,19,40] The OMC has been used as the intermediate in many ethylene oxidation studies,[20–27] where most theoretical investigations used the structure with two Ag atoms.[20–25] In addition to the OMC pathway, a direct epoxidation pathway has been proposed, primarily for a Ag_2O surface mimicking a high oxygen coverage.[39,41,42]

From many previous studies, it is assumed that there are two primary pathways from the OMC: the ring can close to form EO, or H can transfer from C to O to form acetaldehyde (AA), which combusts. The competition between these two pathways is often assumed to control selectivity.[21,43,44] Additional pathways have also been studied.[45] For example, H transfer to the O within the OMC to produce CH_2CHOH has been studied, but found to have a higher barrier than the traditional pathways on Ag(111).[45] With the assistance of machine learning, another possible pathway from the OMC has been reported more recently: H transfer to a hollow site on the Ag surface, eventually leading to AA.[46] This new pathway consists of C–H bond breaking to form 2-oxoethyl and adsorbed H, which can then recombine to form AA or CH_2CHOH. This pathway is thus non-selective and was predicted to have a lower free-energy barrier than the EO and traditional AA pathways.

In industrial practice, the reaction temperature varies from 200 to 300 °C and the pressure from 10 to 30 atm,[7] while conditions used in academic research include wide variations in the ethylene : oxygen ratio as well as a wide range of pressure including ultrahigh vacuum.[7] Catalytically, different ethylene-to-oxygen ratios and overall pressure can have significant effects on the catalytic performance, and can give trade-offs between overall production rates, conversion, and selectivity.[12,13,20,45,47,48] The wide range of conditions in different studies suggests that many different surface states are accessed in these different studies, necessitating an understanding of how reactivity depends on conditions. Many studies examine a low O coverage, such as some ultrahigh vacuum studies and many computational studies; however, these may be quite different from industrial production conditions.[17,19] Some studies have accounted for the oxygen coverage in various ways. Using density functional theory (DFT) calculations, it has been suggested that the barrier for OMC formation strongly depends on the oxygen coverage.[20] Based on experimental studies, Waugh concluded that the selectivity of fully oxidized Ag is determined by the Ag–O bond strength.[22] Reconstructed Ag surfaces induced by high oxygen coverage have been studied experimentally and theoretically, showing that they are not selective in ethylene oxidation.[23] The oxygen coverage has been suggested to be important for selectivity,[49] and O-assisted C–H activation in ethylene has been studied but found to be less favorable than OMC formation.[45] These studies show that the ethylene oxidation mechanism could depend significantly on the oxygen coverage, highlighting the need for further investigation of the role of O in the mechanism.

However, the effect of coadsorbed O on the reactivity of the OMC, or the possible downstream intermediate ethylenedioxy (EDO), has received very little research attention, despite previous work showing that surface O can directly assist surface reactions, including C–H cleavage.[50–52] In this work, we use DFT to systematically study the possible reaction pathways from the OMC in the presence of surface O. We find that surface O opens up two kinetically and thermodynamically favorable pathways, neither of which form EO. Specifically, EDO formation and O-assisted C–H bond scission are quite facile and predicted to far outcompete the previously studied EO (ring closure) and AA (H transfer, either directly within the molecule or *via* the surface) pathways. Furthermore, we studied propylene oxidation on Ag and demonstrated that the oxygen coverage has a similar effect in the propylene-derived OMC. These results suggest that excess atomic O will greatly diminish the selectivity and should be considered in catalyst design.

2. Computational methods

DFT calculations were performed using the Vienna *ab initio* simulation package (VASP).[53,54] The Perdew, Burke, and Ernzerhof generalized gradient functional (GGA-PBE)[55] and the projector augmented-wave (PAW) method[56,57] were used. The Tkatchenko–Scheffler method[58] was used for the dispersion correction. The cutoff energy was set to 400 eV, and a 7 × 7 × 1 *k*-point mesh was used for all the calculations. During the surface relaxations, a 3 × 3 × 4 unit cell was used with the bottom two layers fixed, with a 15 Å vacuum. Dipole corrections were not used. The geometric convergence criterion was set to 0.03 eV Å^{-1}, and the electronic convergence criterion was set to 10^{-5} eV. The transition states were calculated by the dimer[59] method and verified by vibrational frequency calculations. For products that are stable molecules (EO, AA, propylene oxide, and propionaldehyde), we use the gas-phase energies, while for other products we use the adsorbed state energies. The calculated adsorption energies of these species are −0.41, −0.54, −0.47, and −0.46 eV, respectively.

Product probabilities for Fig. 2 were calculated in a simple way, with the free energy barriers and the probability equation $p_i = \frac{\exp\left(\frac{-\Delta G_i}{kT}\right)}{\sum_j \exp\left(\frac{-\Delta G_j}{kT}\right)}$. We calculated rates for Fig. 3 as $r = \theta_O\theta_{OMC}k$ or $r = \theta_{OMC}k$ where θ_{OMC} was set to 1/9 ML in all cases and k is the rate constant determined by DFT. Specifically, we used a linear interpolation of the barrier at 0 monolayers (ML) O and 1/9 ML O to determine the coverage-dependent barrier for reactions that did not explicitly involve O, although this has a negligible effect on the coverage at which the rates are predicted to become similar to each other.

3. Results and discussion

3.1 Ethylene oxidation pathways and products

The OMC is a commonly studied intermediate for ethylene epoxidation, and atomic O may be present on the surface of ethylene epoxidation catalysts under certain reaction conditions.[13] Because it is likely that the OMC and atomic O interact under certain conditions, we studied various reactions of the OMC in the presence of 1/9 ML of O. We examined six pathways from the OMC, two of which have received little or no consideration in previous work.

To start, we examined the reactivity of the OMC under the assumption that the OMC does not directly react with O present on the surface, similar to most previous studies. The most widely studied pathways from the OMC are ring closure to form EO and intramolecular H transfer to form AA. Our calculations predict these two pathways to have very similar barriers, approximately 0.85 eV (see Fig. 1). Of the two, AA has a lower energy in the gas phase by ~1 eV. These results are consistent with previous studies.[27,34,49] Meanwhile, hydrogen transfer to the O atom within the OMC to form vinyl alcohol (VA pathway) gives the lowest energy product, but has the highest barrier of approximately 1.49 eV (~0.6 eV higher than the barriers discussed so far). The same behavior was observed in a previous study,[45] showing that VA formation is kinetically hindered. On the other hand, H can be transferred from the OMC to the surface (H_{surf} pathway) with a barrier of ~0.9 eV, and this C–H scission pathway is expected to be non-selective. This was also shown in a previous study.[49] The H transfer to the surface has a similar barrier to EO and AA, and the energy of the product is between EO and AA, suggesting that this pathway is achievable similar to AA and EO. Overall, these results are similar to previous work, suggesting three pathways with fairly similar barriers, one of which is selective (ring closure, EO pathway) and two of which are nonselective (H transfer to C, AA pathway, and H transfer to the surface, H_{surf} pathway). If we recalculate these barriers without coadsorbed O, we find somewhat lower barriers of 0.74, 0.72, and 0.66 eV for EO, AA, and H_{surf}, respectively, which leads to a similar conclusion.

Next, we studied reactions where the OMC directly reacts with coadsorbed atomic O. We found two pathways which are significantly more thermodynamically and kinetically favorable than any of the previously studied pathways. First, the OMC can react with a coadsorbed O to form ethylenedioxy (EDO).[52,60,61] Our calculations predict a relatively low barrier (~0.5 eV), lower than an early DFT study.[52] This pathway is likely facilitated by the high stability of C–O bonds. Alternatively, the coadsorbed oxygen can promote C–H activation, as has been seen in several other systems.[62–65] Specifically, H can transfer from the OMC to the surface oxygen (OH_{surf} pathway). This pathway has an even lower barrier and reaction energy than the EDO pathway. Previous work shows weakly bound O, such as the O on Ag(111),[66] can greatly facilitate C–H activation in coadsorbed species.[67] These results show that, in the presence of coadsorbed O, the OMC is much more likely to react with O than to go through the traditionally studied pathways. Thus, the importance of the EDO and OH_{surf} pathways may have been neglected in previous studies.

3.2 Product probabilities

The probability of each pathway for the OMC reacting in the presence of coadsorbed O was calculated from 0 to 700 K based on the barriers. Using the calculated free energies of the barriers, the OH_{surf} product has the highest probability, above 99% over the entire temperature range. For example, at a typical reaction temperature of 425 K, OH_{surf} has a probability of 99.90%. The OH_{surf} pathway is expected to be nonselective, indicating very low predicted selectivity from the OMC + O state. Given the possible errors in DFT calculations and the sensitivity of the probabilities to the energy differences, we also tested the inclusion of a 0.2 eV

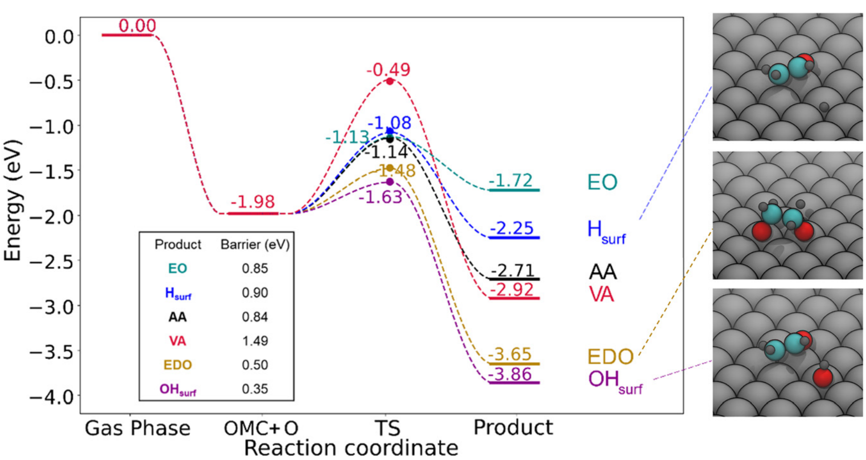

Fig. 1 The calculated reaction energetics for six possible products from the OMC in ethylene oxidation, starting from gas-phase ethylene and $1/2O_2$, proceeding to coadsorbed OMC and O, and undergoing various possible reactions from this state. The final structures for OH_{surf}, EDO, and H_{surf} are shown. EDO formation and O-assisted H abstraction are the most thermodynamically and kinetically favored pathways.

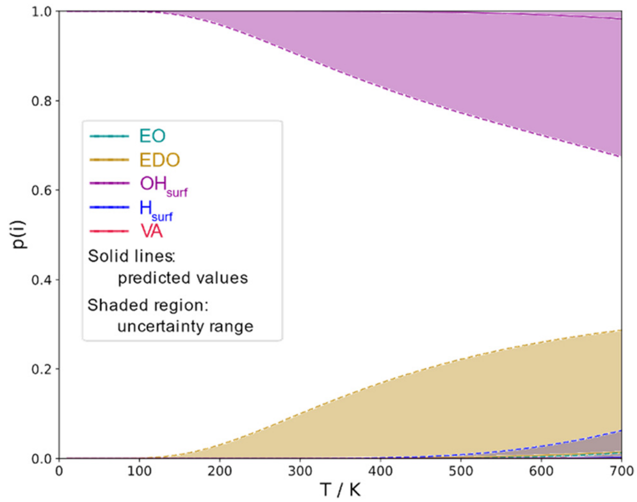

Fig. 2 The calculated probability of each possible product from the OMC based on the reaction free energy barriers. The solid lines use the DFT energetics, and the dotted lines account for a 0.2 eV error in the OH_{surf} barrier.

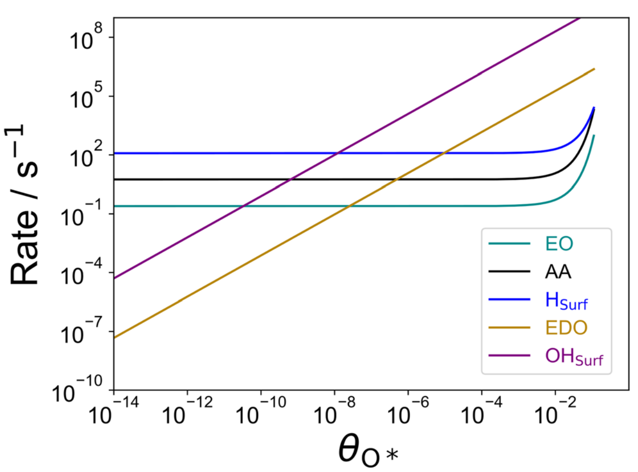

Fig. 3 Calculated rate for various reactions as a function of O coverage, at a temperature of 425 K and a fixed OMC coverage of 1/9 ML.

change in the relative barriers—specifically, the energy of the OH_{surf} barrier was increased by 0.2 eV. Under this scenario, the probability of forming EDO becomes ∼10% at 300 K and ∼30% at 700 K, suggesting the possibility that EDO could build up on the surface. The H_{surf} pathway also shows a nonnegligible probability starting around 400 K and reaches ∼5% at 700 K. The probability of forming EO never reaches above ∼2%, even under this more favorable scenario, indicating that the selectivity is very low for metallic Ag with a significant amount of adsorbed atomic O.

At low O coverage, the rates of O-assisted reactions decrease, such that reactions that do not involve O may still dominate. To estimate the coverage at which O-assisted reactions begin to dominate, we calculated rates as a function of O coverage. These calculations indicate that O-assisted H abstraction may begin to dominate at O coverages as low as 10^{-8} ML. Furthermore, both O-assisted reactions become more favorable than the reactions that do not involve O by 10^{-5} ML. These results are likely somewhat sensitive to errors in DFT, the O mobility, and the kinetic modelling framework, but overall suggest that even quite low coverages of O may be detrimental to the selectivity.

3.3 EDO pathways and products

The EDO intermediate has received relatively little attention for ethylene epoxidation on Ag. Its relative energy was previously calculated by DFT along with other structures such as the OMC.[52] EDO was thermodynamically predicted to form once the oxygen coverage reaches 1/2 ML. However, this previous study also predicted a high barrier to form the second C–O bond in this structure, in contrast to our calculations. EDO has also been studied on Ag–Cu alloys, where it was suggested that the EDO structure is so stable that subsequent reactions from this intermediate are less likely.[60] However, a comprehensive study of its formation and reactivity on Ag is lacking.

Based on the product probabilities, EDO could potentially form at a high enough rate to build up on the surface, and could potentially be an intermediate or a spectator. This raises questions about the selectivity of a pathway that proceeds through EDO and whether it is likely to persist or react. We considered pathways both with and without coadsorbed O. Without coadsorbed O, we considered ring closure to form EO, H transfer between the C atoms in EDO (AA, as a C–O bond breaks simultaneously in this pathway), and H transfer to the surface (H_{surf} pathway). We also considered O-assisted C–H bond scission (OH_{surf} pathway).

In the absence of coadsorbed O, H_{surf} gives the lowest-energy product, while AA formation has the lowest barrier. EO formation is the least favorable pathway, both thermodynamically and kinetically. Thus, EDO does not appear to be an intermediate in selective EO formation. However, all three pathways have very high barriers, suggesting that EDO may persist without reacting for relatively long times in the absence of coadsorbed O. This agrees with the previous studies on CuAg showing that EDO is too stable to react further in the absence of coadsorbed O.[60]

Coadsorbed O can significantly promote C–H bond activation in EDO, whereby the H transfers from the EDO to this coadsorbed O (OH_{surf}). Similar to the O-assisted C–H bond breaking in the OMC, this pathway has a low barrier (0.37 eV) and gives a very stable product. Thus, in the presence of coadsorbed O, EDO is predicted to quickly decompose (Fig. 4).

3.4 Propylene oxidation pathways and products

We performed similar calculations for propylene oxidation to test whether the new pathways we discovered could also be relevant to this system. Some studies have suggested that OMCs may be important in propylene epoxidation,[68] raising the question of whether the trends we saw above for an

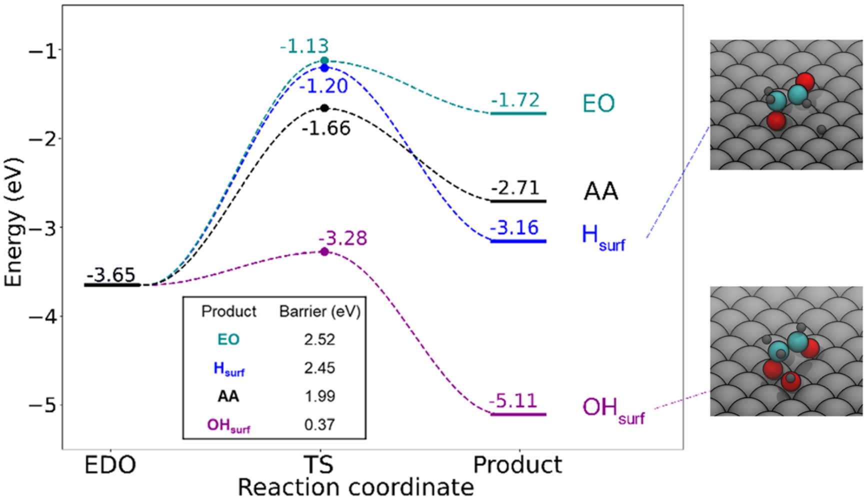

Fig. 4 The calculated reaction energetics for four possible products from EDO. Without coadsorbed O, all reactions are kinetically and thermodynamically unfavorable, but if coadsorbed O is present then O-assisted H abstraction is facile.

ethylene-derived OMC will also apply to a propylene-derived OMC. However, it is important to note that Ag is a poor catalyst for propylene, with low selectivity.[6,69,70] Indeed, the OMC's role in PO is controversial, and some studies have indicated that it does not form because Ag activates the C–H bond of the methyl group.[27,71]

In the propylene oxidation case, the OMC can react to form propylene oxide (PO) or propionaldehyde (PA), neither of which involve direct reaction with coadsorbed O. Alternatively, the OMC can react directly with surface O: H can transfer to the surface oxygen (OH_{surf}) or propylenedioxy (PDO) can form. We performed calculations for all of these pathways, including coadsorbed O at 1/9 ML in all cases. As shown in Fig. 5, although PA still has a lower energy than PO, the barrier for PO formation is 0.13 eV lower than PA. This contrasts with the ethylene oxidation case, where AA had a larger barrier than EO. At higher oxygen coverage, the OH_{surf} pathway has a very low barrier (0.19 eV), suggesting that the H is readily abstracted. However, unlike in the EO case, PDO is the most stable product.

Qualitatively, in the presence of surface O, propylene oxidation pathways have similar trends to ethylene oxidation: O-assisted C–H scission in the OMC is a lower-energy pathway than PO and PA. This again suggests that surface O will lead to nonselective reaction of the propylene-derived OMC, with possible implications for the overall reaction selectivity not only for PO, but possibly other epoxidation reactions as well.

4. Discussion

Overall, we can conclude that surface atomic O has high reactivity in assisting C–H bond activation in both the OMC and EDO. This is consistent with the experimental findings

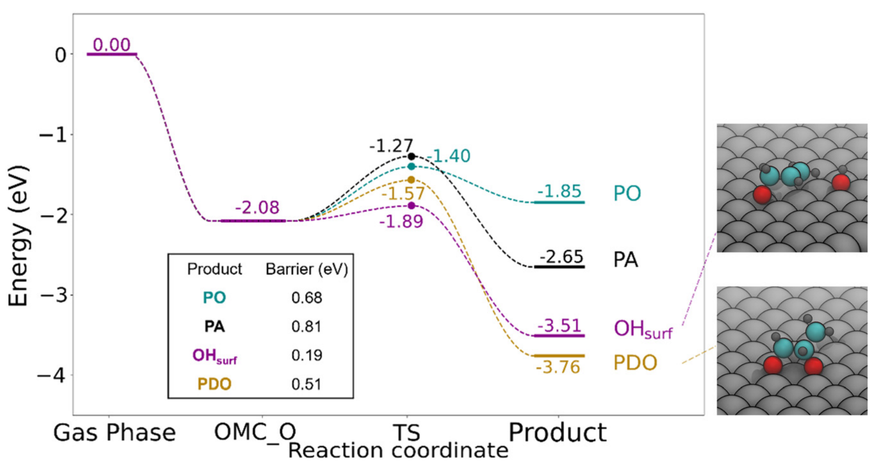

Fig. 5 The calculated reaction energetics for four possible products from the OMC in propylene oxidation. Similar to ethylene epoxidation, PDO formation and O-assisted H abstraction are the most thermodynamically and kinetically favorable pathways.

that, at high oxygen coverage, EO selectivity increases with a higher ethylene pressure as this would likely reduce the amount of surface atomic O.[48] Similarly, experimental studies often suggest that Cl reduces the presence of surface atomic O.[33,72]

Some previous studies indicate that the Ag surface is quite oxidized under certain conditions,[12,15,28] in contrast to the metallic surface considered here and in most computational studies. It is likely that a metallic surface persists under other conditions, particularly those with a higher ethylene : oxygen ratio and/or at a higher temperature, and it is these conditions that are most directly relevant to our study.

5. Conclusions

This study provides a detailed, DFT-based analysis of the impact of coadsorbed atomic O on epoxidation reaction pathways. Our findings reveal that surface O significantly affects selectivity, opening up the nonselective pathways of EDO formation and O-assisted C–H bond scission, which are both kinetically and thermodynamically more favorable than traditional EO and AA pathways. These pathways dominate when coadsorbed O is present, greatly reducing the predicted overall selectivity towards EO from roughly 50% in the traditional picture to roughly 0.1%. These insights underline the critical importance of controlling surface oxygen coverage in EO production. Similar trends observed in propylene oxidation support the possible applicability of these findings to other alkene epoxidations. Consequently, surface oxygen coverage may be a critical factor to consider when designing selective catalysts for EO and related processes.

Data availability

Data for this article are given in the figures and text.

Conflicts of interest

There are no conflicts to declare.

Acknowledgements

We acknowledge support from the U.S. – Israel Center for Fossil Fuels, administered by the BIRD foundation. This work was also supported by the National Science Foundation through grant CBET-2340356. The authors acknowledge support from Tulane University, in part using high-performance computing (HPC) resources and services provided by Technology Services at Tulane University. Some portions of this research were conducted with HPC resources provided by the Louisiana Optical Network Infrastructure (https://www.loni.org).

References

1 O. US EPA, Ethylene oxide CASRN 75-21-8 | DTXSID0020600 | IRIS | US EPA, ORD, https://cfpub.epa.gov/ncea/iris2/chemicalLanding.cfm?substance_nmbr=1025, (accessed 1 March 2024).
2 Fact.MR – Ethylene Oxide Market Analysis by Application (Ethylene Glycol, Ethoxylates, Ethanolamines, Glycol Esters, Polyethylenes) and by Region – Global Forecast 2022–2032, https://www.factmr.com/report/ethylene-oxide-market, (accessed 1 March 2024).
3 Ethylene oxide global market volume 2015–2030 | Statista, https://www.statista.com/statistics/1245260/ethylene-oxide-market-volume-worldwide/, (accessed 1 March 2024).
4 S. Rebsdat and D. Mayer, in *Ullmann's Encyclopedia of Industrial Chemistry*, ed. Wiley-VCH, Wiley, 1st edn, 2001.
5 G. Sienel, R. Rieth and K. T. Rowbottom, in *Ullmann's Encyclopedia of Industrial Chemistry*, John Wiley & Sons, Ltd, 2000.
6 T. A. Nijhuis, M. Makkee, J. A. Moulijn and B. M. Weckhuysen, *Ind. Eng. Chem. Res.*, 2006, **45**, 3447–3459.
7 T. Pu, H. Tian, M. E. Ford, S. Rangarajan and I. E. Wachs, *ACS Catal.*, 2019, **9**, 10727–10750.
8 J. Teržan, M. Huš, B. Likozar and P. Djinović, *ACS Catal.*, 2020, **10**, 13415–13436.
9 J. Lu, J. J. Bravo-Suárez, A. Takahashi, M. Haruta and S. T. Oyama, *J. Catal.*, 2005, **232**, 85–95.
10 P. Christopher and S. Linic, *ChemCatChem*, 2010, **2**, 78–83.
11 A. J. F. van Hoof, E. A. R. Hermans, A. P. van Bavel, H. Friedrich and E. J. M. Hensen, *ACS Catal.*, 2019, **9**, 9829–9839.
12 C. Liu, D. P. Wijewardena, A. Sviripa, A. Sampath, D. W. Flaherty and C. Paolucci, *J. Catal.*, 2022, **405**, 445–461.
13 M. O. Özbek and R. A. van Santen, *Catal. Lett.*, 2013, **143**, 131–141.
14 C. J. Keijzer, L. C. J. Smulders, D. Wezendonk, J. W. de Rijk and P. E. de Jongh, *Catal. Today*, 2024, **428**, 114447.
15 T. Pu, A. Setiawan, B. Mosevitzky Lis, M. Zhu, M. E. Ford, S. Rangarajan and I. E. Wachs, *ACS Catal.*, 2022, **12**, 4375–4381.
16 G. S. Jones, M. Mavrikakis, M. A. Barteau and J. M. Vohs, *J. Am. Chem. Soc.*, 1998, **120**, 3196–3204.
17 S. Linic and M. A. Barteau, *J. Am. Chem. Soc.*, 2002, **124**, 310–317.
18 S. Linic and M. A. Barteau, *J. Am. Chem. Soc.*, 2003, **125**, 4034–4035.
19 S. Linic and M. A. Barteau, *J. Catal.*, 2003, **214**, 200–212.
20 A. Kokalj, P. Gava, S. De Gironcoli and S. Baroni, *J. Phys. Chem. C*, 2008, **112**, 1019–1027.
21 A. Kokalj, P. Gava, S. de Gironcoli and S. Baroni, *J. Catal.*, 2008, **254**, 304–309.
22 K. C. Waugh and M. Hague, *Catal. Today*, 2010, **157**, 44–48.
23 T. E. Jones, R. Wyrwich, S. Böcklein, T. C. R. Rocha, E. A. Carbonio, A. Knop-Gericke, R. Schlögl, S. Günther, J. Wintterlin and S. Piccinin, *J. Phys. Chem. C*, 2016, **120**, 28630–28638.
24 L. Zhu, W. Zhang, J. Zhu and D. Cheng, *Appl. Catal., A*, 2017, **538**, 27–36.
25 E. A. Carbonio, T. C. R. Rocha, A. Y. Klyushin, I. Píš, E. Magnano, S. Nappini, S. Piccinin, A. Knop-Gericke, R. Schlögl and T. E. Jones, *Chem. Sci.*, 2018, **9**, 990–998.

26 H. Xu, L. Zhu, Y. Nan, Y. Xie and D. Cheng, *ACS Catal.*, 2021, **11**, 3371–3383.
27 M. Huš and A. Hellman, *ACS Catal.*, 2019, **9**, 1183–1196.
28 T. Pu, A. Setiawan, A. C. Foucher, M. Guo, J.-M. Jehng, M. Zhu, M. E. Ford, E. A. Stach, S. Rangarajan and I. E. Wachs, *ACS Catal.*, 2024, **14**, 406–417.
29 J.-X. Liu, S. Lu, S.-B. Ann and S. Linic, *ACS Catal.*, 2023, **13**, 8955–8962.
30 J. T. Jankowiak and M. A. Barteau, *J. Catal.*, 2005, **236**, 379–386.
31 J. T. Jankowiak and M. A. Barteau, *J. Catal.*, 2005, **236**, 366–378.
32 J. C. Dellamorte, J. Lauterbach and M. A. Barteau, *Catal. Today*, 2007, **120**, 182–185.
33 T. C. R. Rocha, M. Hävecker, A. Knop-Gericke and R. Schlögl, *J. Catal.*, 2014, **312**, 12–16.
34 L. Zhu, H. Xu, Y. Nan, Y. Xie, J. Zhu and D. Cheng, *Appl. Surf. Sci.*, 2019, **476**, 115–122.
35 M. A. Salaev, A. A. Salaeva and O. V. Vodyankina, *Catal. Today*, 2021, **375**, 585–590.
36 B. W. J. Chen, B. Wang, M. B. Sullivan, A. Borgna and J. Zhang, *ACS Catal.*, 2022, **12**, 2540–2551.
37 K. R. Iyer and A. Bhan, *J. Catal.*, 2024, **436**, 115583.
38 A. Jalil, E. E. Happel, L. Cramer, A. Hunt, A. S. Hoffman, I. Waluyo, M. M. Montemore, P. Christopher and E. C. H. Sykes, *Science*, 2025, **387**, 869–873.
39 M. Urbiztondo, A. Ramirez, J. L. Hueso, J. Santamaria, A. Rabdel Ruiz-Salvador and S. Hamad, *Nanoscale*, 2022, **14**, 7332–7340.
40 J. W. Medlin and M. A. Barteau, *J. Phys. Chem. B*, 2001, **105**, 10054–10061.
41 M. O. Özbek, I. Önal and R. A. van Santen, *ChemCatChem*, 2011, **3**, 150–153.
42 A. Kokalj, A. Dal Corso, S. de Gironcoli and S. Baroni, *J. Phys. Chem. B*, 2006, **110**, 367–376.
43 M. M. Montemore and J. W. Medlin, *J. Phys. Chem. C*, 2014, **118**, 2666–2672.
44 G. O. Kayode and M. M. Montemore, *J. Mater. Chem. A*, 2021, **9**, 22325–22333.
45 M. O. Ozbek, I. Onal and R. A. van Santen, *Top. Catal.*, 2012, **55**, 710–717.
46 D. Chen, P.-L. Kang and Z.-P. Liu, *ACS Catal.*, 2021, **11**, 8317–8326.
47 M. M. Montemore, M. A. van Spronsen, R. J. Madix and C. M. Friend, *Chem. Rev.*, 2018, **118**, 2816–2862.
48 A. V. Khasin, *React. Kinet. Catal. Lett.*, 1998, **64**, 289–294.
49 M. Huš, M. Grilc, J. Teržan, S. Gyergyek, B. Likozar and A. Hellman, *Angew. Chem., Int. Ed.*, 2023, **62**, e202305804.
50 I. Rivalta, G. Mazzone, N. Russo and E. Sicilia, *Chem. Phys. Lett.*, 2010, **493**, 87–93.
51 P. T. Lachkov and Y.-H. Chin, *J. Catal.*, 2018, **366**, 127–138.
52 J. Greeley and M. Mavrikakis, *J. Phys. Chem. C*, 2007, **111**, 7992–7999.
53 G. Kresse and J. Hafner, *Phys. Rev. B: Condens. Matter Mater. Phys.*, 1993, **47**, 558–561.
54 G. Kresse and J. Furthmüller, *Comput. Mater. Sci.*, 1996, **6**, 15–50.
55 J. P. Perdew, K. Burke and Y. Wang, *Phys. Rev. B: Condens. Matter Mater. Phys.*, 1996, **54**, 16533–16539.
56 P. E. Blöchl, *Phys. Rev. B: Condens. Matter Mater. Phys.*, 1994, **50**, 17953–17979.
57 G. Kresse and D. Joubert, *Phys. Rev. B: Condens. Matter Mater. Phys.*, 1999, **59**, 1758–1775.
58 A. Tkatchenko and M. Scheffler, *Phys. Rev. Lett.*, 2009, **102**, 073005.
59 G. Henkelman and H. Jónsson, *J. Chem. Phys.*, 1999, **111**, 7010–7022.
60 N. L. Nguyen, S. Piccinin and S. de Gironcoli, *J. Phys. Chem. C*, 2011, **115**, 10073–10079.
61 S. Piccinin, N. Linh Nguyen, C. Stampfl and M. Scheffler, *J. Mater. Chem.*, 2010, **20**, 10521–10527.
62 C.-Q. Lv, J.-H. Liu, J. Ren and G.-C. Wang, *Int. J. Hydrogen Energy*, 2018, **43**, 17048–17056.
63 H. Wang, C. He, L. Huai and J. Liu, *J. Phys. Chem. C*, 2013, **117**, 4574–4584.
64 C. G. F. Siler, T. Cremer, J. C. F. Rodriguez-Reyes, C. M. Friend and R. J. Madix, *ACS Catal.*, 2014, **4**, 3281–3288.
65 T. Cremer, C. G. F. Siler, J. C. F. Rodríguez-Reyes, C. M. Friend and R. J. Madix, *J. Phys. Chem. Lett.*, 2014, **5**, 1126–1130.
66 W.-X. Li, C. Stampfl and M. Scheffler, *Phys. Rev. B: Condens. Matter Mater. Phys.*, 2002, **65**, 075407.
67 J. S. Yoo, T. S. Khan, F. Abild-Pedersen, J. K. Nørskov and F. Studt, *Chem. Commun.*, 2015, **51**, 2621–2624.
68 Y. Dai, Z. Chen, Y. Guo, G. Lu, Y. Zhao, H. Wang and P. Hu, *Phys. Chem. Chem. Phys.*, 2017, **19**, 25129–25139.
69 M. B. Burkholder, M. M. Rahman, A. C. Reber, A. M. Gaffney, B. F. Gupton and J. R. Monnier, *Appl. Catal., A*, 2023, **650**, 119002.
70 J. R. Monnier, *Appl. Catal., A*, 2001, **221**, 73–91.
71 B. Zhao and G.-C. Wang, *J. Phys. Chem. C*, 2019, **123**, 17273–17282.
72 C. J. Keijzer, P. T. Weide, K. H. Helfferich, J. Zieciak, M. de Ridder, R. Dalebout, T. L. Lohr, J. R. Lockemeyer, P. van den Brink and P. E. de Jongh, *Catal. Sci. Technol.*, 2025, **15**, 323–333.